NON-LINEAR STRUCTURAL ANALYSIS OF SHEAR FLEXIBLE FGM BEAMS

K. Sanjay Anandrao, R.K. Gupta
Scientist
Advanced Systems Laboratory
Kanchanbagh
Hyderabad-500 058, India

P. Ramachandran
Scientist
Defence Research and Development Laboratory
Kanchanbagh
Hyderabad-500 058, India

G. Venkateswara Rao
Research Professor
Department of Mechanical Engineering
Vardhaman College of Engineering, Shamshabad
Hyderabad-501 218, India
Email : hydrao1944@yahoo.co.in

Abstract

Non-linear structural response of Functionally Graded Material (FGM) beams is studied using the finite element method. The deformations obtained using Euler-Bernoulli beam and Timoshenko beam theories are compared for different length to height ratios, volume fraction exponents and boundary conditions. The percentage errors in lateral deformations for neglecting the effects of shear flexibility are discussed in detail. Through thickness variation of the axial stress shows a shift in the neutral axis from the mid-thickness of beam for homogenous as well as FGM beams and for the boundary conditions considered. The range of volume fraction exponents for the practical design of FGM beams is suggested to avoid steep stress gradients.

Keywords*: shear flexibility, von-Karman geometric non-linearity, FGM beam, finite element method, Newton-Raphson method, iterative solution*

Nomenclature

b	= Width of beam
$f(x)$	= Generalized axial load
h	= Thickness of beam
n	= Volume fraction exponent
n_x	= Direction cosine of the unit normal on the element boundary l^e
$q(x)$	= Generalized transverse load
u	= Deformation along x-axis
w	= Deformation along z axis
x	= Coordinate along length of beam
z	= Coordinate along thickness of the beam
A_{11}	= Extensional stiffness
A_{55}	= Shear stiffness
B_{11}	= Extension-bending coupling stiffness
D_{11}	= Bending stiffness
E	= Effective modulus of elasticity of FGM
E_m	= Modulus of elasticity of metal
E_c	= Modulus of elasticity of ceramic
F	= Element load vector
G	= Shear modulus
K	= Element stiffness matrix
K_s	= Shear correction factor
L	= Length of beam
M_{xx}	= Moment resultant
N_{xx}	= Stress resultant
Q_x	= Shear stress resultant
R	= Residual
T	= Tangent stiffness matrix
V	= Transverse shear
V_m	= Volume fraction of metal

Paper Code : V64 N2/765-2012. Manuscript received on 28 Nov 2011. Reviewed and accepted as a Full Length Contributed Paper on 16 Jan 2012

V_c = Volume fraction of ceramic
ε_{xx} = Axial strain
σ_{xx} = Axial stress
δu_0, δw_0 = Virtual displacements
ϕ = Rotation
$\delta\phi$ = Virtual rotation
γ_{xz} = Transverse shear strain
τ_{xz} = Transverse shear stress
ψ_i = Lagrange interpolation functions

Introduction

Japanese scientists proposed the concept of Functionally Graded Materials (FGM) as a means of preparing thermal barrier materials (Koizumi [1]). In FGM, the micro-structural details of the constituent materials are continuously varied spatially (Aboudi [2]) to obtain the desired distribution of properties such as Young's modulus, thermal conductivity etc. The choice of these constituent materials is governed by the intended application of the FGM structure.

Slender FGM beams and columns can be used as structural members in a variety of structural applications such as advanced aircraft and aerospace engines, re-entry vehicles, computer circuit boards, automobile, nuclear components, steel plants etc. Unlike homogenous structures, the design of FGM structures is controlled by many variables. Development and understanding of appropriate modeling techniques are required to fully utilize their potential. For the mass sensitive applications as found in aerospace components, accurate evaluation of deflections and stresses is very important to realize optimized structures.

Static analysis of FGM beams has been reported in the literature, mostly by analytical methods. Sankar [3] proposed an elasticity solution for Euler-Bernoulli type FGM beams, where an exponential variation of Young's modulus was assumed through the thickness. Deschilder [4] presented an analytical model to study the non-linear static analysis of the FGM beam. In this work, the governing differential equations were developed and solved for various boundary conditions. An analytical solution of a cantilever FGM beam was proposed by Zhong [5] in terms of Airy stress function. Thermal post-buckling analysis of FGM beams was studied by Thivend [6] wherein a closed form solution was obtained by solving the governing differential equations. A beam with simply supported and axially immovable edges was considered to obtain deflections from pre-buckling to post-buckling temperatures. Anandrao [7, 8] studied the pre-buckling and post-buckling response of FGM beams using the non-linear finite element method as well as the Rayleigh-Ritz method. They considered FGM beams with axially immovable ends with simply supported as well as clamped boundary conditions. A non-linear static analysis of uniform slender FGM beams was presented by Anandrao [9] using the finite element method. They established non-linear load-deformation paths for various boundary conditions. A new unified approach was presented by Li [10] for studying the static and dynamic behavior of FGM beams wherein shear deformation and rotary inertia was included and in which an arbitrary variation of material properties was considered through the thickness. Chakraborty [11] developed a new beam finite element based on first order shear deformation theory to study static, free vibration and wave propagation analysis of functionally graded material beam structures. Ying [12] analyzed functionally graded material beams resting on a Winkler-Pasternak elastic foundation. They studied the bending and free vibrations of FG beams based on two dimensional elasticity theory. The material properties were assumed to vary exponentially through the thickness. Kapuria [13] used third order zigzag theory to evaluate the effective modulus of elasticity and studied the static and free vibration response of layered FG beams. Kadoli [14] presented the static analysis of FG beams by using the higher order shear deformation theory and finite element method. Benatta [15] studied the bending of symmetric FG beam by including the warping of the cross section and the shear deformation effect. Sallai [16] studied the static response of a sigmoid FG thick beam by using various beam theories.

In this paper, a detailed study of the structural response of shear flexible homogenous and through-thickness functionally graded uniform beams subjected to a uniformly distributed lateral load is presented using the finite element method, based on Euler-Bernoulli beam and Timoshenko beam theories. The Simply supported and clamped beams with axially immovable ends are considered. Geometric non-linearity is considered using von-Kármán strain-displacement relations, where moderately large deflections of the order of the characteristic dimension of the cross section of the beam are allowed. Young's modulus is assumed to vary according to a power law distribution across the thickness. The governing non-linear equations are obtained using the principle of virtual work. Newton-Raphson iterative procedure is used to solve these non-linear equations wherein the load is applied in increments. The formulation is validated by comparing the results with those obtained from the finite

element software ANSYS® [17] for homogenous beams for the boundary conditions considered. The present work also discusses about the limits on the choice of volume fraction exponent in the strength based design of FGM structures. A detailed study pertaining to the deflection and stress variation of FGM beams, subjected to transverse load, which is important in the strength based design of FGM structures, and the error involved by neglecting the shear flexibility, is summarized here.

Functionally Graded Material Beam

A through-thickness functionally graded material beam with ceramic on top face and metal on bottom face is considered in the present study. The variation of Young's modulus and shear modulus across thickness is governed by a power law distribution, given in Equation (1), with the thickness co-ordinate varying between -*h*/2 to *h*/2. The volume fraction exponent can take any value between 0 to ∞ where the value of 0 corresponds to pure ceramic and value tending to ∞ corresponds to pure metal. The chosen value of *n* for a typical application will decide the property variations and response of FGM beam.

$$\left.\begin{aligned} E(z) &= E_c V_c + E_m (1 - V_c) \\ V_c &= \left(0.5 + \frac{z}{h}\right)^n \end{aligned}\right\} \quad (1)$$

Finite Element Formulation

Displacement Field - Nodal Displacement Relation

Two separate beam formulations, one neglecting shear flexibility effects (Euler-Bernoulli) and the other considering shear flexibility effects (Timoshenko) are developed. The details of Euler-Bernoulli beam theory are available from Anandrao [9]. The details of Timoshenko beam formulation are presented here. A beam element with two nodes per element and three degrees of freedom per node is considered. Using Lagrange linear interpolation functions for axial displacement, lateral displacement and rotation, the degrees of freedom vector for a Timoshenko beam element can be written as

$$\left.\begin{aligned} u(x) &= \psi_1 u_1 + \psi_2 u_2 \\ w(x) &= \psi_1 w_1 + \psi_2 w_2 \\ \phi(x) &= \psi_1 \phi_1 + \psi_2 \phi_2 \end{aligned}\right\} \quad (2)$$

Strain-Displacement Relations

By considering von-Kármán type geometric non-linearity, where moderately large rotations and displacements of the order of characteristic dimension of the cross section of the beam are considered, the strain-displacement relations can be written as

$$\varepsilon_{xx} = \frac{du_0}{dx} + \frac{1}{2}\left(\frac{dw_0}{dx}\right)^2 - z\frac{d\phi_x}{dx} \quad (3)$$

The additional term in the axial strain accounts for the stretching of mid-plane due to the transverse displacement. The transverse shear strain is given by

$$\gamma_{xz} = \phi_x + \frac{dw_0}{dx} \quad (4)$$

Stress-Strain Equation

The axial stress is related to axial strain by equation

$$\sigma_{xx} = E(z)\,\varepsilon_{xx} \quad (5)$$

The transverse shear stress is related to transverse shear strain by equation

$$\tau_{xx} = G(z)\,\gamma_{xz} \quad (6)$$

Stress and Moment Resultant-Displacement Relations

The stress resultant and moment resultant in the axial direction can be expressed as,

$$\left.\begin{aligned} N_{xx} &= \left[\frac{du_0}{dx} + \frac{1}{2}\left(\frac{dw_0}{dx}\right)^2\right] A_{11} + \frac{d\phi_x}{dx} B_{11} \\ M_{xx} &= \left[\frac{du_0}{dx} + \frac{1}{2}\left(\frac{dw_0}{dx}\right)^2\right] B_{11} + \frac{d\phi_x}{dx} D_{11} \end{aligned}\right\} \quad (7)$$

where

$$\left.\begin{aligned} A_{11} &= \int_{-h/2}^{h/2} E(z)\,dz \\ B_{11} &= \int_{-h/2}^{h/2} E(z)\,z\,dz \\ D_{11} &= \int_{-h/2}^{h/2} E(z)\,z^2\,dz \end{aligned}\right\} \quad (8)$$

and shear stress resultant is

$$Q_x = K_s A_{55} \left(\frac{dw_0}{dx} + \phi_x \right) \tag{9}$$

where shear stiffness is

$$A_{55} = \int_{-h/2}^{h/2} G(z)\, dz \tag{10}$$

Governing Differential Equations

The differential equations governing the bending of initially straight beams are

$$\left.\begin{aligned} -\frac{dN_{xx}}{dx} + f(x) &= 0 \\ -\frac{dQ_x}{dx} - \frac{d}{dx}\left(N_{xx}\frac{dw_0}{dx}\right) - q(x) &= 0 \\ -\frac{dM_{xx}}{dx} + Q_x &= 0 \end{aligned}\right] \tag{11}$$

Weak Form

The finite element system of equations to study the non-linear behavior of FGM beam can be derived by using principle of virtual work. The weak forms of governing differential equations can be obtained from Reddy [18, 19] as given in Eq. (12).

$$\int_{\Omega^e} \frac{d(\delta u_0)}{dx} \left\{ \left[\frac{du_0}{dx} + \frac{1}{2}\left(\frac{dw_0}{dx}\right)^2 \right] A_{11} + \frac{d\phi_x}{dx} B_{11} \right\} dx - \oint_{\Gamma^e} N_n\, \delta u_0\, ds = 0$$

$$\int_{\Omega^e} K_s \frac{d(\delta w_0)}{dx} A_{55} \left(\frac{dw_0}{dx} + \phi_x \right) dx$$

$$+ \int_{\Omega^e} \frac{d(\delta w_0)}{dx} \left\{ \frac{dw_0}{dx} A_{11} \left[\frac{du_0}{dx} + \frac{1}{2}\left(\frac{dw_0}{dx}\right)^2 \right] + B_{11}\frac{d\phi_x}{dx} \right\} dx$$

$$- \delta w_0\, q dx - \oint_{\Gamma^e} V_n\, \delta w_0\, ds = 0$$

$$\int_{\Omega^e} \frac{d(\delta \phi_x)}{dx} B_{11} \left[\frac{du_0}{dx} + \frac{1}{2}\left(\frac{dw_0}{dx}\right)^2 \right] + D_{11}\frac{d\phi_x}{dx}$$

$$+ K_s\, \delta\phi_x A_{55} \left(\frac{dw_0}{dx} + \phi_x \right) dx - \oint_{\Gamma^e} M_n\, \delta\phi_n\, ds = 0 \tag{12}$$

where

$$N_n = N_{xx} n_x$$

$$V_n = Q_n + \frac{dM_{ns}}{ds} + P$$

$$M_n = M_{xx} n_x$$

$$P = N_{xx} \frac{dw_0}{dx} n_x \tag{13}$$

The virtual work statement above contains at the most only the first derivatives of the dependent variables. They can all be approximated using Lagrange interpolation functions as given in Equation (2). Substituting expressions for u, w and ϕ from Equation (2) in the weak form and rearranging, the finite element system of equations can be expressed as,

$$\begin{bmatrix} [K^{11}] & [K^{13}] & [K^{14}] \\ [K^{31}] & [K^{33}] & [K^{34}] \\ [K^{41}] & [K^{43}] & [K^{44}] \end{bmatrix} \begin{Bmatrix} \{u^e\} \\ \{w^e\} \\ \{\phi^e\} \end{Bmatrix} = \begin{bmatrix} F^1 \\ F^3 \\ F^4 \end{bmatrix} \tag{14}$$

For Timoshenko beam elements, when linear interpolation of the lateral deflection and rotation is used, the elements do not accurately represent the bending behavior as length to thickness ratio becomes large. For slender beams, the transverse shear strain is required to vanish and the beam elements with linear interpolation become excessively stiff, giving rise to shear locking. In the present study, the phenomenon of shear locking is alleviated by evaluating stiffness coefficients associated with transverse shear deformation using reduced integration and full integration is used for all other stiffness coefficients. For example, in $[K^{44}]$, the stiffness term containing A_{55} requires 2-point numerical integration to evaluate the integral exactly. However, this term is evaluated by using 1-point numerical integration to avoid shear locking.

Newton-Raphson Solution

The element system of equations from Equation (14) can be assembled to obtain non-linear finite element system of equations of the form

$$K(U)\,U = F \tag{15}$$

Newton-Raphson iterative method is used for solving non-linear Equation (15). The residual at the end of any iteration r can be defined as

$$R = KU - F \tag{16}$$

Load step is given in terms of increment from the previous converged solution. Using Newton-Raphson algorithm, for the r^{th} iteration,

$$U^{r+1} = U^{r} - (T^{r})^{-1} R^{r} \tag{17}$$

where the tangent stiffness matrix is given by

$$T^{r} = \frac{\partial R^{r}}{\partial U} \tag{18}$$

The iterative procedure is terminated when the Euclidean norm of the residual vectors (L_2) is lower than the specified tolerance ε ($1\text{x}10^{-4}$).

$$\sqrt{\sum_{i=1}^{n} R_i^2} \le \varepsilon \tag{19}$$

Results and Discussion

A FGM beam with the material properties is given in Table-1 is considered for this study. A code was developed in MATLAB based on the above formulation.

A typical FGM beam with a thickness of 3 mm and varying lengths was considered. The beam was discretized with 100 equal length elements. A transverse uniformly distributed load of 200 N/mm was applied in 10 equal sub steps. A shear correction factor Ks = 5/6 was considered in this study.

Table-1 : Material Properties of Ceramic and Metal

Property	Ceramic	Metal
Young's Modulus E (MPa)	375000	70000
Poisson's Ratio v	0.3	0.3

Simply Supported Beam (SS)

Figure 1 shows comparison of normalized lateral deformation $\bar{W}$ ($= W_{\max} E_m h^3/q L^4$) at the mid length of the ceramic beam for L/h = 10 with the normalized load $\bar{q}$ ($= q L^4/E_c h^4$) obtained from linear and non-linear analysis using Timoshenko beam formulation. The effect of non-linearity can be clearly observed which justifies the need for the non-linear analysis when the beam undergoes large deformations. Further, hardening type of non-linearity is observed as the stiffness of the structure increases with load.

Table-2 shows a comparison of the normalized maximum lateral deflection for homogenous beam obtained from the present formulations and ANSYS with various L/h ratios. Deflections are obtained without including the shear flexibility (Euler-Bernoulli beam) and with including the shear flexibility (Timoshenko beam). A very good correlation is observed between the results obtained using the present formulations and ANSYS.

The study is further extended using the present formulations for the analysis of FGM beam. The lateral deformations obtained for various L/h ratios are summarized in Table-3a and 3b.

As expected, at lower values of ratio L/h, a large difference was observed in the central deflection obtained without considering and with considering shear flexibility. At higher values of ratio L/h, the effect of shear flexibility on the deformation of beam is negligible. Table-4 shows the percentage error in central deflection when the shear effects are neglected.

For homogenous simply supported beam with axially immovable ends, shear effects can be neglected after L/h

Table-2 : $\overline{W}$ (x 100) at Mid Length of SS Homogeneous Beam

L/h	$n = 0$ (Present) Euler	Ceramic (ANSYS) Euler	$n = 0$ (Present) Timoshenko	Ceramic (ANSYS) Timoshenko
5	2.8931	2.8940	3.1728	3.1777
10	1.6973	1.7022	1.7086	1.7243
20	0.3389	0.3407	0.3390	0.3411
50	0.0301	0.0304	0.0301	0.0304
100	0.0047	0.0048	0.0047	0.0048

Table-3a : $\overline{W}$ (x 100) at Mid Length of SS FGM Beam						
L/h	*n* = 0 Euler	*n* = 0 Timoshenko	*n* = 0.5 Euler	*n* = 0.5 Timoshenko	*n* = 1.0 Euler	*n* = 1.0 Timoshenko
5	2.8931	3.1728	3.9329	4.2623	4.5280	4.8983
10	1.6973	1.7086	1.8216	1.8335	1.9262	1.9397
20	0.3389	0.3390	0.3636	0.3636	0.3846	0.3848
50	0.0301	0.0301	0.0331	0.0331	0.0353	0.0353
100	0.0047	0.0047	0.0053	0.0053	0.0056	0.0056

Table-3b : $\overline{W}$ (x 100) at Mid Length of SS FGM Beam						
L/h	*n* = 2.0 Euler	*n* = 2.0 Timoshenko	*n* = 10.0 Euler	*n* = 10.0 Timoshenko	*n* = 100.0 Euler	*n* = 100.0 Timoshenko
5	5.1944	5.6433	7.3851	8.1319	11.8630	12.7071
10	2.0934	2.1103	2.7196	2.7391	3.4588	3.4638
20	0.4169	0.4173	0.5143	0.5146	0.5911	0.5912
50	0.0384	0.0384	0.0466	0.0466	0.0519	0.0519
100	0.0061	0.0061	0.0074	0.0074	0.0082	0.0082

Table-4 : % Error in Maximum Lateral Deflection for Neglecting Shear Effects (SS Beam)						
L/h	*n* = 0 Euler	*n* = 0.5 Euler	*n* = 1.0 Euler	*n* = 2.0 Euler	*n* = 10.0 Euler	*n* = 100.0 Euler
5	8.8133	7.7297	7.5607	7.9551	9.1842	6.6428
10	0.6623	0.6490	0.6977	0.8016	0.7113	0.1448
20	0.0301	0.0080	0.0455	0.0909	0.0510	0.0234
50	0.0000	0.0056	0.0264	0.0486	0.0320	0.0036
100	0.0000	0.0062	0.0166	0.0305	0.0205	0.0000

≥ 50. For FGM beams, however, a small difference in lateral deflection can be observed even at higher values of *L/h* ratio. This necessitates consideration of shear flexibility in the analysis of FGM beam even at higher values of *L/h* ratio. Very high values of *n* (≥ 100) correspond to homogenous beam (completely metal) and is expected to show lower errors at *L/h* ≥ 50 like *n* = 0.

Figure 2 shows the variation of the normalized maximum lateral deformation at mid length with the normalized load $\overline{q}$ for several volume fraction exponents for *L/H*=10. As the volume fraction is increased, the lateral deformation of the beam increases.

Figure 3 shows through the thickness variation of the normalized axial stress ($\sigma_{xx} h^2/L^2 q$) at the mid-length with different volume fraction exponents for *L/h* = 10. The Neutral Axis (NA) is not at the mid-thickness for both homogenous as well as FGM beams and is given in Table-5. Further, for the homogenous beam (*n* = 0.0), the axial stress variation is linear through the thickness. For FGM beams, however, the axial stress variation is not linear. For *n* = 0.5, the maximum tensile stress does not

Table-5 : Depth of Neutral Axis for SS FGM Beam						
	$n = 0$	$n = 0.5$	$n = 1.0$	$n = 2.0$	$n = 10.0$	$n = 100.0$
Depth of NA (z / h)	0.042215	0.022215	0.00841	-0.00363	0.03855	0.119901

occur at the bottom surface but slightly inside the thickness. On the other hand, for $n \geq 2.0$, a steep gradient in stress occurs near the top surface. These large variations in stress can be avoided by limiting the volume fraction exponent between $0.0 \geq n \geq 2.0$ in the practical design.

Figure 4 and 5 shows the variation of the normalized lateral and axial deformation along the length at q = 200 N/mm and L/h = 10 for various volume fraction exponents. It is observed that as the volume fraction increases, the deformation of the FGM beam increases.

Clamped Beam (CC)

A similar study is carried out for homogenous and FGM beams with clamped ends. Fig.6 shows comparison of $\overline{W}$ at mid length of ceramic beam for L/h = 20 obtained from linear and non-linear analysis. Hardening type of non-linearity is observed for this boundary condition. Table-6 shows comparison of normalized maximum lateral deflection at mid length. A very good correlation is observed between the results obtained using present formulations and ANSYS for homogenous beams.

The lateral deformations obtained using the present formulation for various L/h ratios of FGM beam are summarized in Tables-7a and 7b.

Similar to the beam with simply supported ends, at lower values of ratio L/h, large difference is observed for the central deflection obtained without and with considering the shear flexibility. Table-8 shows the percentage error in the central lateral deflection when the effects of the transverse shear are neglected.

Table-6 : $\overline{W}$ (x 100) at Mid Length of CC Homogeneous Beam				
L/h	$n = 0$ (Present) Euler	Ceramic (ANSYS) Euler	$n = 0$ (Present) Timoshenko	Ceramic (ANSYS) Timoshenko
5	0.5833	0.5833	0.8742	0.8744
10	0.5721	0.5723	0.6391	0.6415
20	0.2733	0.2741	0.2769	0.2799
50	0.0290	0.0292	0.0291	0.0294
100	0.0047	0.0047	0.0047	0.0048

The % error in lateral deflection for neglecting shear effects is found to be much higher for clamped beam as compared to simply supported beam. Even at higher values of L/h ratio, shear flexibility has effect on central deflection.

Figure 7 shows variation of normalized maximum lateral deformation with normalized load for various volume fraction exponents for L/h = 20. As the volume fraction is increased, the lateral deformation of the beam increases. Fig.8 shows the through thickness variation of normalized axial stress ($\sigma_{xx} h^2/L^2 q$) at mid-length with different volume fraction exponents for L/h = 20. As observed for the simply supported beam, the neutral axis is not at the mid-thickness for both the homogenous as well as FGM beams. The location of neutral axis is given in Table-9. Further, for the homogenous beam (n = 0.0), the axial stress variation is linear through the thickness but for FGM beams, the axial stress variation is not linear.

Figure 9 and 10 shows the variation of the normalized lateral deformation and the axial deformation along the length of the beam for q = 200 N/mm and L/h = 20 for various volume fraction exponents. As the volume fraction increases, the deformation of the FGM beam increases.

Transverse Shear Stress Variation

Based on the Timoshenko beam theory, the shear strain variation is constant through the thickness. In the present study, the differential equation of equilibrium for plane problems Equation (20) is used to obtain the variation of transverse shear stress τ_{xz} through the thickness.

$$\frac{\partial \sigma_{xx}}{\partial x} + \frac{\partial \tau_{xz}}{dz} = 0 \qquad (20)$$

Table-7a : $\overline{W}$ (x 100) at Mid Length of CC FGM Beam						
L/h	$n = 0$ Euler	$n = 0$ Timoshenko	$n = 0.5$ Euler	$n = 0.5$ Timoshenko	$n = 1.0$ Euler	$n = 1.0$ Timoshenko
5	0.5833	0.8742	0.8979	1.2966	1.1652	1.6544
10	0.5721	0.6391	0.8561	0.9388	1.0772	1.1689
20	0.2733	0.2769	0.3233	0.3269	0.3560	0.3597
50	0.0290	0.0291	0.0325	0.0326	0.0349	0.0350
100	0.0047	0.0047	0.0052	0.0052	0.0056	0.0056

Table-7b : $\overline{W}$ (x 100) at Mid Length of CC FGM Beam						
L/h	$n = 2.0$ Euler	$n = 2.0$ Timoshenko	$n = 10.0$ Euler	$n = 10.0$ Timoshenko	$n = 100.0$ Euler	$n = 100.0$ Timoshenko
5	1.4887	2.1218	1.9286	3.0389	2.7871	4.2635
10	1.3267	1.4327	1.6843	1.8571	2.2005	2.3765
20	0.3955	0.3999	0.4808	0.4849	0.5426	0.5505
50	0.0381	0.0383	0.0460	0.0463	0.0509	0.0512
100	0.0061	0.0061	0.0074	0.0074	0.0081	0.0082

Table-8 : % Error in Maximum Lateral Deflection for Neglecting Shear Effects (CC Beam)						
L/h	$n = 0$ Euler	$n = 0.5$ Euler	$n = 1.0$ Euler	$n = 2.0$ Euler	$n = 10.0$ Euler	$n = 100.0$ Euler
5	33.2780	30.7501	29.5735	29.8399	36.5356	34.6278
10	10.4801	8.8157	7.8461	7.3941	9.3039	7.4080
20	1.2695	1.0974	1.0519	1.0923	1.4616	1.4279
50	0.4035	0.4180	0.4326	0.4707	0.6196	0.6222
100	0.2167	0.2343	0.2483	0.2727	0.3520	0.3390

Table-9 : Depth of Neutral Axis for CC FGM Beam						
	$n = 0$	$n = 0.5$	$n = 1.0$	$n = 2.0$	$n = 10.0$	$n = 100.0$
Depth of NA (z / h)	0.075554	0.027908	0.00831	-0.00233	0.065954	0.208238

The top face (*h/2*) and bottom face (*-h/2*) are free of shear tractions. By integrating Equation (20), the transverse shear stress at any depth can be obtained.

To validate the transverse shear stresses obtained using Equation (20), a plane stress analysis was carried out using the commercial finite element software ANSYS. A clamped beam with $L/h = 10$ was modeled using PLANE42 elements (2 DOF, u_x and u_y). The ANSYS idealization of the structure is as shown in Fig.11 where-in both DOF are set to zero at two ends of the structure. The number of elements used to idealize the length-wise beam

cross-section are 30 in along the length and 20 along the thickness (or depth) of the beam. A geometric non-linear analysis is carried out for the completely homogenous structure.

Figure 12 shows typical through thickness variation of axial stress obtained using present study (Timoshenko) and ANSYS plane stress analysis at $L = 9$ mm. A very good match can be observed between the two results. Further, it can be observed that the location of the zero axial stress (Neutral Axis) is not at the mid-thickness.

Figure 13 shows through thickness variation of transverse shear stress obtained using present study with Equation (20) and ANSYS plane stress analysis at $L = 9$ mm. Again, a very good match is observed between the two results.

The present study is further extended for FGM beams using Equation (20). A typical variation of transverse shear stress through thickness for FGM beam is shown in Fig.14. For homogenous beam ($n = 0$ and $n = 100$), the shear stress variation is parabolic and the maximum value occurs at mid-thickness. For FGM beam, however, the shear stress variation is governed by the variation of shear modulus through the thickness and the maximum transverse shear stress occurs at location other than mid-thickness.

Conclusions

A detailed non-linear analysis of shear flexible FGM beams subjected to uniformly distributed lateral load is presented. Finite element formulations, based on Euler-Bernoulli beam and Timoshenko beam theories are separately developed. The following conclusions can be drawn from this study.

- Shear flexibility effects play a dominant role for lower values of length to height ratios and should be considered to obtain a realistic response.
- The effect of the shear flexibility is found to be much higher for clamped beam as compared to simply supported beam.
- It is observed that for large deformations, the neutral axis does not remain at the mid-thickness for the homogenous as well as FGM beams.
- A steep stress gradient is observed through the thickness for higher values of volume fraction exponents for FGM beams.

Acknowledgements

The authors are thankful to the managements of their respective organizations for the encouragement during the course of this work.

References

1. Koizumi, M., "The Concept of FGM", Ceram. Trans., Vol.34, No.1, 1993, pp.3-10.

2. Aboudi, J., Pindera, M. J. and Arnold, S. M., "Higher Order Theory for Functionally Graded Materials", Composites Part B-Engineering, 1999, Vol.30, pp.777-832.

3. Sankar, B. V., "An Elasticity Solution for Functionally Graded Beams", Composites Science and Technology, 2001, Vol. 61, pp.689-696.

4. Deschilder, M., Eslami, H. and Zhao, Y., "Non-linear Static Analysis of a Beam Made of Functionally Graded Material", AIAA-2011, 2006, pp.1-9.

5. Zhong, Z. and Tao, Y., "Analytical Solution of a Cantilever Functionally Graded Beam", Composites Science and Technology, 2007, Vol. 67, pp.481-488.

6. Thivend, J., Eslami, H. and Zhao, Y., "Thermal Post Buckling Analysis of FGM Beams", AIAA-2272, 2008, pp.1-21.

7. Anandrao, S. K., Gupta, R. K., Ramchandran, P. and Rao, G.V., "Thermal Post-buckling Analysis of Uniform Slender Functionally Graded Material Beams Using Non-linear Finite Element Method", International Congress on Computational Mechanics and Simulation, Indian Institute of Technology Bombay, India, 2009.

8. Anandrao, S. K., Gupta, R.K., Ramchandran, P. and Rao, G.V., "Thermal Post-buckling Analysis of Uniform Slender Functionally Graded Material Beams", Structural Engineering and Mechanics, An International Journal, 2010, Vol.36, No.5, pp.545-560.

9. Anandrao, S. K., Gupta, R. K., Ramchandran, P. and Rao, G.V., "Non-linear Static Analysis of Uniform Slender Functionally Graded Material Beams Using Finite Element Method", Proc. Nat. Acad. Sci. India, 2011, Vol.81, pp.71-78.

10. Li, X. F., "A Unified Approach for Analyzing Static and Dynamic Behaviors of Functionally Graded Timoshenko and Euler-Bernoulli Beams", Journal of Sound and Vibration, 2008, Vol. 318, pp.1210-1229.

11. Chakraborty, A., Gopalkrishnan, S. and Reddy, J. N., "A New Beam Finite Element for the Analysis of Functionally Graded Materials", International Journal of Mechanical Sciences, 2003, Vol.45, No.3, pp.519-539.

12. Ying, J., Lu, C.F. and Chen, W. Q., "Two-dimensional Elasticity Solutions for Functionally Graded Beams Resting on Elastic Foundations", Composite Structures, 2008, Vol.84, No.3, pp.209-219.

13. Kapuria, S., Bhattacharyya, M. and Kumar, A. N., "Bending and Free Vibration Response of Layered Functionally Graded Beams: A Theoretical Model and its Experimental Validation", Composite Structures, 2008, Vol. 82, No. 3, pp.390-402.

14. Kadoli, R., Akthar, K. and Ganesan, N., "Static Analysis of Functionally Graded Beams Using Higher Order Shear Deformation Theory", Applied Mathematical Modelling, 2008, Vol.32, No.12, pp.2509-2525.

15. Benatta, M. A., Mechab, I., Tounsi, A. and Adda Bedia, E. A., "Static Analysis of Functionally Graded Short Beams Including Warping and Shear Deformation Effects", Computational Materials Science, 2008, Vol.44, No.2, pp.765-773.

16. Sallai, B. O., Tounsi, A., Mechab, I., Bachir, B. M., Meradjah, M. and Adda, B.E. A., "A Theoretical Analysis of Flexional Bending of Al/Al_2O_3 S-FGM Thick Beams", Computational Materials Science, 2009, Vol.44, No.4, pp.1344-1350.

17. ANSYS Inc. ANSYS Package Version 10.0, Canons Burgh, PA, USA.

18. Reddy, J.N., "Mechanics of Laminated Composite Plates and Shells: Theory and Analysis", CRC Press, New York, 2003.

19. Reddy, J.N., "An Introduction to Non-linear Finite Element Analysis", Oxford University Press, USA, 2004.

Appendix

$$K_{ij}^{11} = \int_{\Omega^e} A_{11} \frac{d\psi_i}{dx} \frac{d\psi_j}{dx} dx$$

$$K_{ij}^{13} = \frac{1}{2} \int_{\Omega^e} \frac{d\psi_i}{dx} A_{11} \frac{dw_0}{dx} \frac{d\psi_j}{dx} dx$$

$$K_{ij}^{14} = \int_{\Omega^e} \frac{d\psi_i}{dx} B_{11} \frac{d\psi_j}{dx} dx = K_{ji}^{41}$$

$$K_{ij}^{31} = \int_{\Omega^e} \frac{d\psi_j}{dx} A_{11} \frac{dw_0}{dx} \frac{d\psi_i}{dx} dx$$

$$K_{ij}^{33} = K_s \int_{\Omega^e} \frac{d\psi_i}{dx} A_{55} \frac{d\psi_j}{dx} dx + \frac{1}{2} \int_{\Omega^e} A_{11} \left(\frac{dw_0}{dx}\right)^2 \frac{d\psi_i}{dx} \frac{d\psi_j}{dx} dx$$

$$K_{ij}^{34} = K_s \int_{\Omega^e} A_{55} \frac{d\psi_i}{dx} \psi_j dx + \int_{\Omega^e} \frac{d\psi_i}{dx} \frac{dw_0}{dx} B_{11} \frac{d\psi_j}{dx} dx$$

$$K_{ij}^{43} = K_s \int_{\Omega^e} A_{55} \frac{d\psi_i}{dx} \psi_j dx + \frac{1}{2} \int_{\Omega^e} \frac{d\psi_j}{dx} \frac{dw_0}{dx} B_{11} \frac{d\psi_i}{dx} dx$$

$$K_{ij}^{44} = \int_{\Omega^e} \frac{d\psi_i}{dx} D_{11} \frac{d\psi_j}{dx} + K_s A_{55} \psi_i \psi_j dx$$

$$F_i^1 = \oint_{\Gamma^e} N_{xx} \psi_i ds$$

$$F_i^3 = \int_{\Omega^e} q \psi_i dx$$

$$F_i^4 = \oint_{\Gamma^e} M_{xx} \psi_i ds$$

$$T_{ij}^{11} = K_{ij}^{11}$$

$$T_{ij}^{13} = 2K_{ij}^{13} = T_{ji}^{31}$$

$$T_{ij}^{14} = K_{ij}^{14}$$

$$T_{ij}^{33} = \int_{\Omega^e} \frac{du_0}{dx} A_{11} \frac{d\psi_j}{dx} \frac{d\psi_i}{dx} dx + \int_{\Omega^e} A_{11} \frac{dw_0}{dx} \frac{d\psi_j}{dx} \frac{d\psi_i}{dx} \frac{dw_0}{dx} dx$$

$$\int_{\Omega^e} \frac{d\psi_i}{dx} \frac{d\psi_j}{dx} B_{11} \frac{d\phi_x}{dx} dx + K_{ij}^{33}$$

$$T_{ij}^{34} = K_{ij}^{34}$$

$$T_{ij}^{41} = K_{ij}^{41}$$

$$T_{ij}^{43} = \frac{1}{2} \int_{\Omega^e} \frac{dw_0}{dx} \frac{d\psi_j}{dx} B_{11} \frac{d\psi_i}{dx} dx + K_{ij}^{43}$$

$$T_{ij}^{44} = K_{ij}^{44}$$

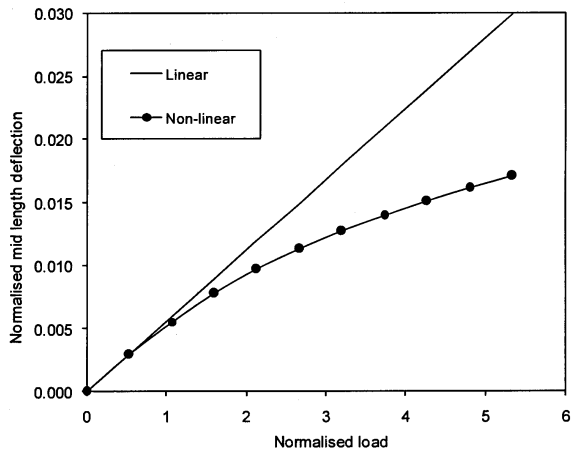

Fig.1 $\overline{W}$ at Mid Length of SS Homogenous Beam (n = 0, L/h = 10)

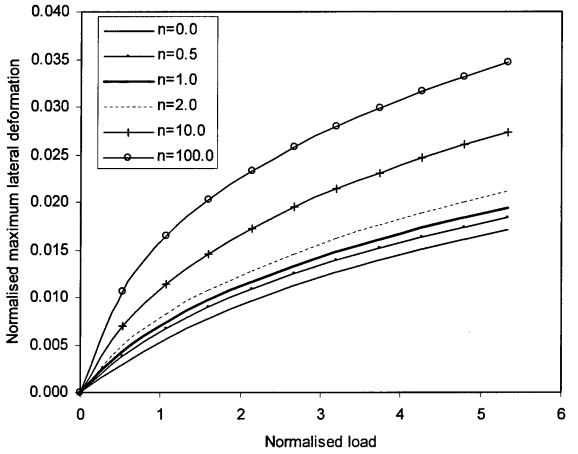

Fig.2 Normalised Lateral Deformation at Mid Length of SS FGM Beam (L/h = 10)

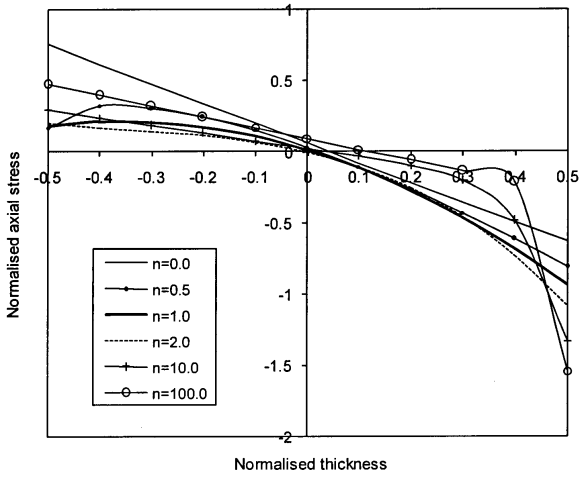

Fig.3 Through Thickness Variation of Normalised Axial Stress at Mid-length of SS FGM Beam, q = 40 N/mm, L/h = 10

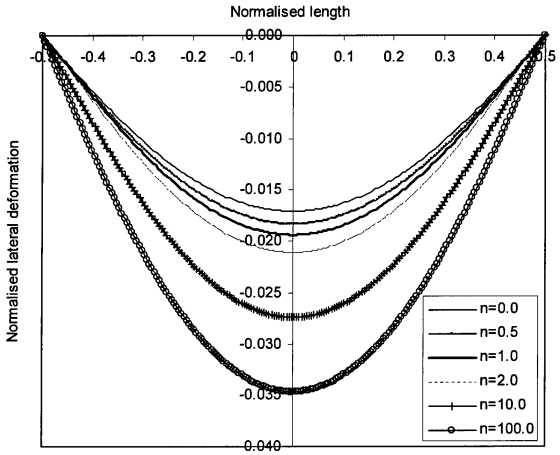

Fig.4 Normalised Lateral Deformation ($WE_mh^3/q\,L^4$) Along Length of SS FGM Beam (L/h = 10)

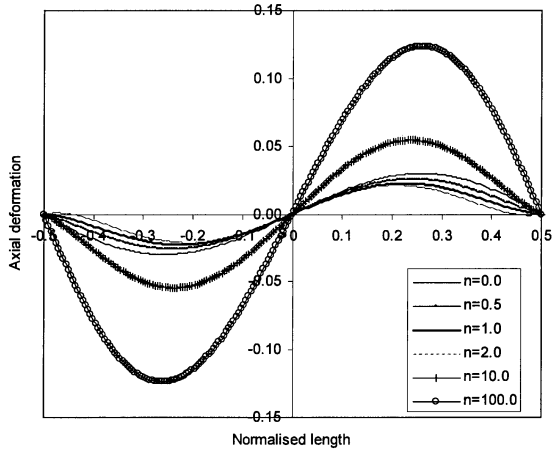

Fig.5 Axial Deformation Along Length of SS FGM Beam (L/h = 10)

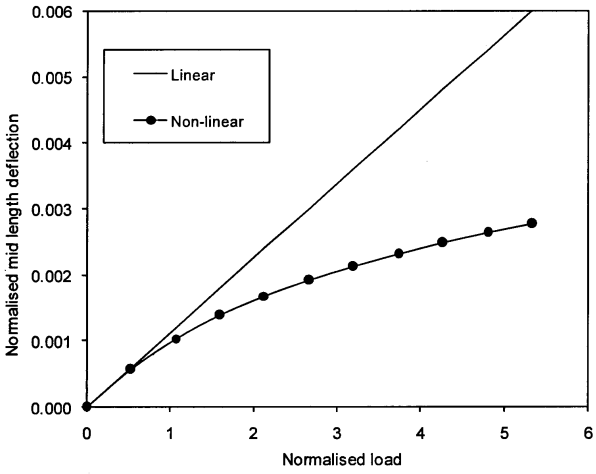

Fig.6 Normalised Lateral Deformation at Mid Length of CC Homogenous Beam (n = 0, L/h = 20)

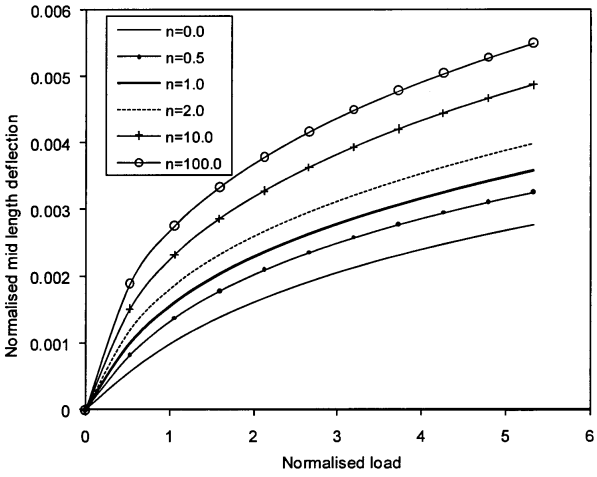

Fig.7 Normalised Lateral Deformation at Mid Length of CC FGM Beam (L/h = 20)

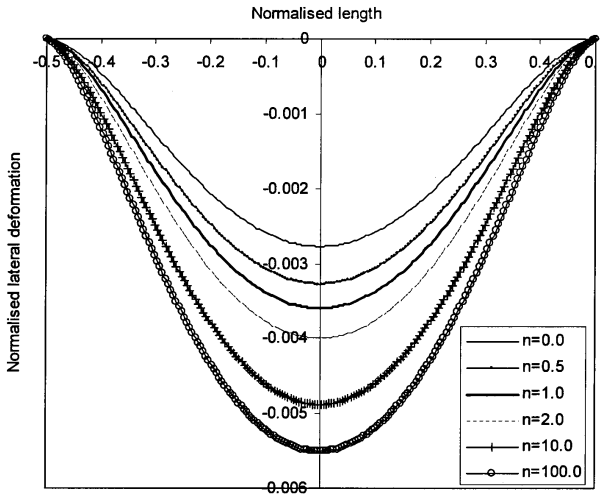

Fig.9 $\overline{W}$ Along Length of CC FGM Beam (L/h = 20)

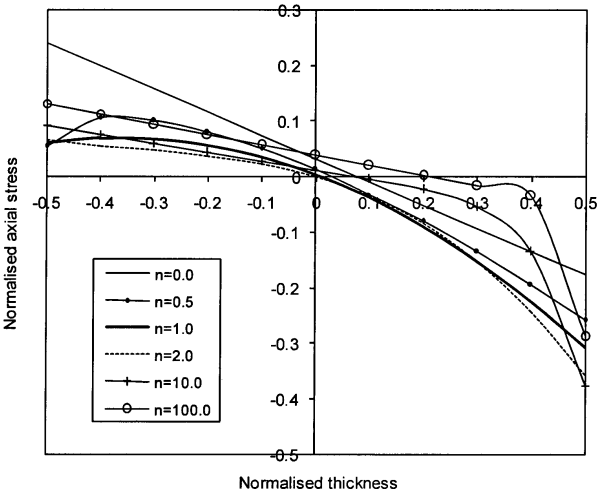

Fig.8 Through Thickness Variation of Normalised Axial Stress at Mid-length of CC FGM Beam, q = 40 N/mm, L/h = 20

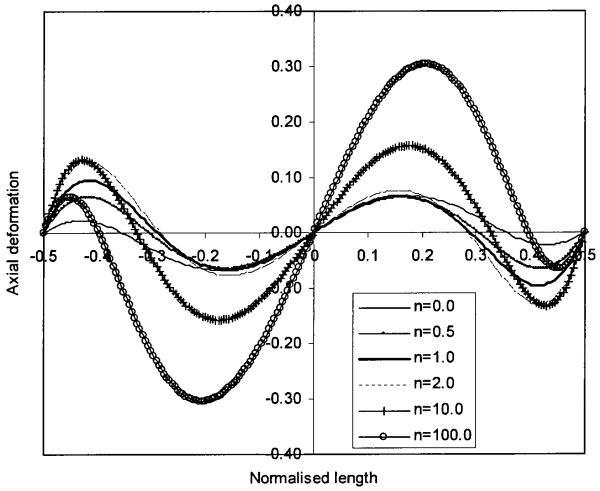

Fig.10 Axial Deformation Along Length of CC FGM Beam (L/h = 20)

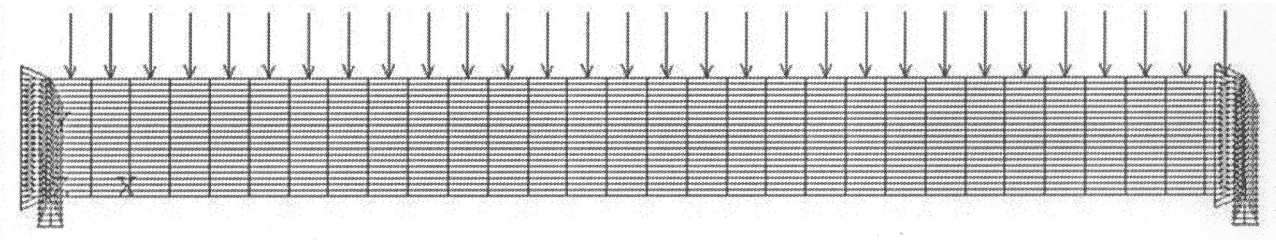

Fig.11 Plane Stress Idealisation of Clamped Homogenous Structure (q = 200 N/mm, L/h = 10)

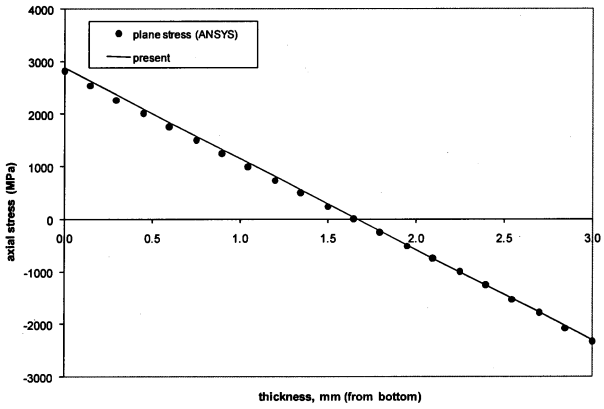

Fig.12 Comparison of Axial Stress Variation Through Thickness, ANSYS (Plane Stress) and Present (q = 200 N/m, L/h = 10)

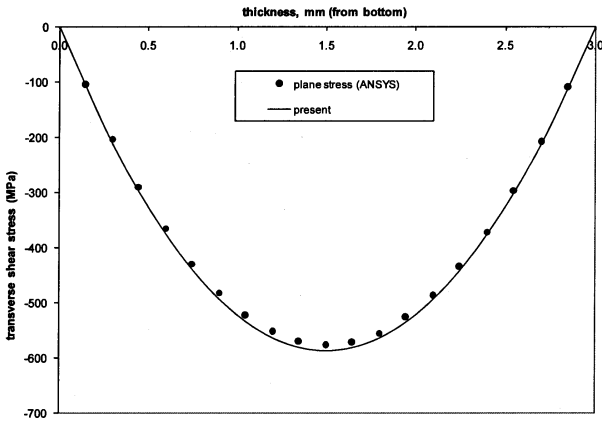

Fig.13 Comparison of Transverse Shear Stress Variation Through Thickness, ANSYS (Plane Stress) and Present (Equation 20) (q = 200 N/m, L/h = 10)

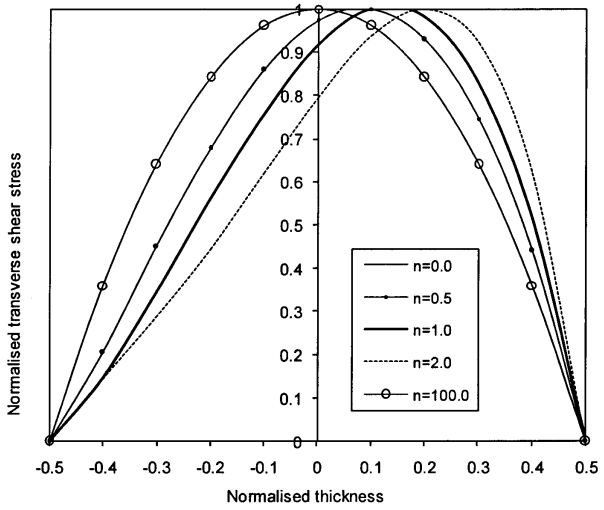

Fig.14 Typical Through Thickness Variation of Normalised Transverse Shear Stress ($\tau_{xz}h/bq$) for SS FGM Beam (q = 200 N/mm, L/h = 10)